EPJ C direct
electronic only

Status of neutrino masses and mixing

Carlo Giunti

INFN, Sezione di Torino, and Dipartimento di Fisica Teorica, Università di Torino, Via P. Giuria 1, I–10125 Torino, Italy

Abstract. The experimental evidences in favor of oscillations of solar (and KamLAND) and atmospheric (and K2K) neutrinos are briefly reviewed and accommodated in the framework of three-neutrino mixing. The implications for the values of neutrino masses are discussed and the bounds on the absolute scale of neutrino masses from Tritium β-decay and cosmological data are reviewed. Finally, we discuss the implications of three-neutrino mixing for neutrinoless double-β decay.

PACS. 14.60.Lm – 14.60.Pq – 26.65.+t – 95.85.Ry

About one year ago, the observation of solar neutrinos through neutral-current and charged-current reactions allowed the SNO experiment [1] to solve the long-standing solar neutrino problem in favor of the existence of $\nu_e \to \nu_\mu, \nu_\tau$ transitions. The global analysis of all solar neutrino data in terms of the most natural hypothesis of neutrino oscillations favored the so-called Large Mixing Angle (LMA) region with a squared-mass difference $2 \times 10^{-5} \lesssim \Delta m^2_{\mathrm{SUN}} \lesssim 4 \times 10^{-4}$ (we measure squared-mass differences in units of eV^2) and a large effective mixing angle $0.2 \lesssim \tan^2 \vartheta \lesssim 0.9$ (see [2]). A spectacular proof of the correctness of the LMA region has been obtained at the end of last year in the KamLAND long-baseline $\bar{\nu}_e$ disappearance experiment [3], in which a suppression of $0.611 \pm 0.085 \pm 0.041$ of the $\bar{\nu}_e$ flux produced by nuclear reactors at an average distance of about 180 km was observed. The allowed regions of the effective neutrino oscillation parameters obtained from the global analysis of solar and KamLAND neutrino data are shown in Fig. 1 [4]. The effective squared-mass difference $\Delta m^2_{\mathrm{SUN}}$ is constrained in one of the two ranges [5]

$$\text{LMA-I:} \quad 5.1 \times 10^{-5} < \Delta m^2_{\mathrm{SUN}} < 9.7 \times 10^{-5}, \quad (1a)$$

$$\text{LMA-II:} \quad 1.2 \times 10^{-4} < \Delta m^2_{\mathrm{SUN}} < 1.9 \times 10^{-4}, \quad (1b)$$

at 99.73% C.L., with best-fit value $\Delta m^{2\,\mathrm{bf}}_{\mathrm{SUN}} \simeq 6.9 \times 10^{-5}$ in the LMA-I region (see also [2] and references therein). The effective solar mixing angle ϑ_{SUN} is constrained at 99.73% C.L. in the interval [5]

$$0.29 < \tan^2 \vartheta_{\mathrm{SUN}} < 0.86, \quad (2)$$

with best-fit value $\tan^2 \vartheta^{\mathrm{bf}}_{\mathrm{SUN}} \simeq 0.46$.

Transitions of solar ν_e's into sterile states are disfavored by the data. Figure 2 [6] shows the allowed regions in the $f_{\mathrm{B,total}}$–$\sin^2 \eta$ plane, where $f_{\mathrm{B,total}} = \Phi_{\mathrm{8B}}/\Phi^{\mathrm{SSM}}_{\mathrm{8B}}$ is the ratio of the ^{8}B solar neutrino flux and its value
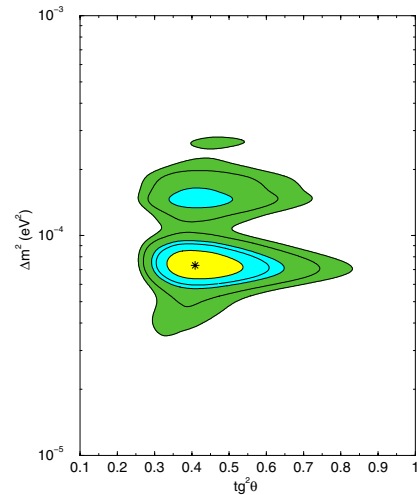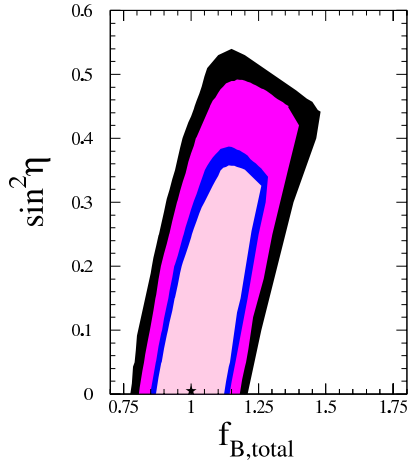

Fig. 1. Allowed 68.3%, 90%, 95%, 99%, 99.73% C.L. regions obtained from the global analysis of solar and KamLAND data. The best-fit point is marked by a star. Figure from [4].

predicted by the Standard Solar Model (SSM) [7]. The parameter $\sin^2 \eta$ quantifies the fraction of solar ν_e's that transform into sterile ν_s: $\nu_e \to \cos \eta \, \nu_a + \sin \eta \, \nu_s$, where ν_a are active neutrinos. From Fig. 2 it is clear that there is a correlation between $f_{\mathrm{B,total}}$ and $\sin^2 \eta$, which is due to the constraint on the total flux of ^{8}B active neutrinos given by the SNO neutral-current measurement: disappearance into sterile states is possible only if the ^{8}B solar neutrino flux is larger than the SSM prediction. The allowed ranges for Φ_{8B} and $\sin^2 \eta$ are [6]

$$\Phi_{\mathrm{8B}} = 1.00 \pm 0.06 \, \Phi^{\mathrm{SSM}}_{\mathrm{8B}}, \quad \sin^2 \eta < 0.52. \quad (3)$$

The allowed interval for Φ_{8B} shows a remarkable agreement of the data with the SSM, independently from possible $\nu_e \to \nu_s$ transitions.

Fig. 2. Allowed 90%, 95%, 99%, 99.73% C.L. regions obtained from the global analysis of solar and KamLAND data. The best-fit point is marked by a star. Figure from [6].
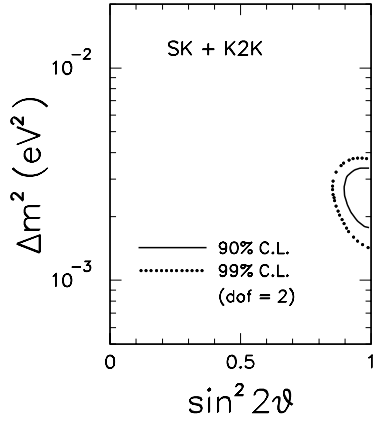
Fig. 3. Allowed region obtained from the analysis of Super-Kamiokande atmospheric and K2K data in terms of $\nu_\mu \to \nu_\tau$ oscillations. Figure from [12].

In the future it is expected that the KamLAND experiment will allow to distinguish between the LMA-I and LMA-II regions, reaching a relatively high accuracy in the determination of $\Delta m^2_{\mathrm{SUN}}$ [8], whereas new low-energy solar neutrino experiments or a new dedicated reactor neutrino experiment are needed in order to improve significantly our knowledge of the solar effective mixing angle ϑ_{SUN} [9–11].

In 1998 the Super-Kamiokande Collaboration [13] discovered the up-down asymmetry of high-energy events generated by atmospheric ν_μ's, providing a model independent proof of atmospheric ν_μ disappearance. At the end of 2002 the long-baseline K2K experiment [14] confirmed the neutrino oscillation interpretation of the atmospheric neutrino anomaly observing the disappearance of accelerator ν_μ's at a distance of 250 km from the source. The data of atmospheric and K2K experiments are well fitted by $\nu_\mu \to \nu_\tau$ transitions generated by the squared-mass difference $\Delta m^2_{\mathrm{ATM}}$ in the 99.73% C.L. range [12]
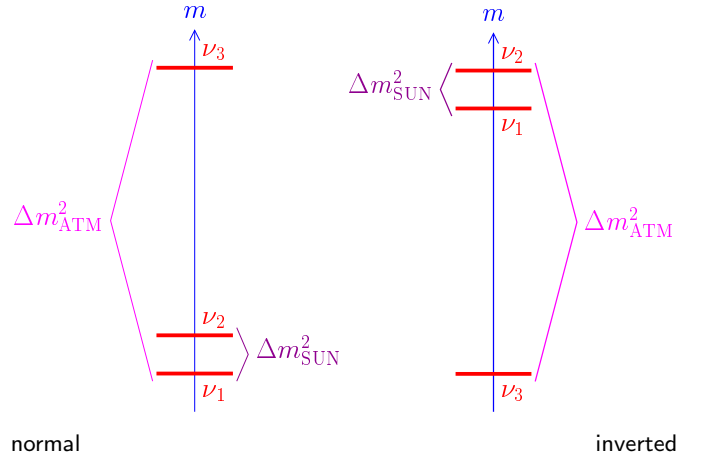
Fig. 4. The two three-neutrino schemes allowed by the hierarchy $\Delta m^2_{\mathrm{SUN}} \ll \Delta m^2_{\mathrm{ATM}}$.

$$1.4 \times 10^{-3} < \Delta m^2_{\mathrm{ATM}} < 5.1 \times 10^{-3} , \qquad (4)$$

with best-fit value $\Delta m^{2\,\mathrm{bf}}_{\mathrm{ATM}} \simeq 2.6 \times 10^{-3}$. The best-fit effective atmospheric mixing is maximal, $\sin^2 2\vartheta^{\mathrm{bf}}_{\mathrm{ATM}} \simeq 1$, with the 99.73% C.L. lower bound [12]

$$\sin^2 2\vartheta_{\mathrm{ATM}} > 0.86 . \qquad (5)$$

Figure 3 [12] shows the allowed region obtained from the analysis of Super-Kamiokande atmospheric and K2K data.

Transitions of atmospheric ν_μ's into ν_e's or sterile states are disfavored. The fraction $\sin^2 \xi$ of atmospheric ν_μ's that transform into sterile ν_s ($\nu_\mu \to \cos \xi \, \nu_\tau + \sin \xi \, \nu_s$) is limited by [15]

$$\sin^2 \xi < 0.19 \quad (90\% \text{ C.L.}) . \qquad (6)$$

The solar and atmospheric evidences of neutrino oscillations are nicely accommodated in the minimal framework of three-neutrino mixing, in which the three flavor neutrinos ν_e, ν_μ, ν_τ are unitary linear combinations of three neutrinos ν_1, ν_2, ν_3 with masses m_1, m_2, m_3, respectively (see [16]). Figure 4 shows the two three-neutrino schemes allowed by the observed hierarchy of squared-mass differences, $\Delta m^2_{\mathrm{SUN}} \ll \Delta m^2_{\mathrm{ATM}}$, with the massive neutrinos labeled in order to have

$$\Delta m^2_{\mathrm{SUN}} = \Delta m^2_{21} , \quad \Delta m^2_{\mathrm{ATM}} \simeq |\Delta m^2_{31}| \simeq |\Delta m^2_{32}| . \quad (7)$$

The two schemes in Fig. 4 are usually called "normal" and "inverted", because in the normal scheme the smallest squared-mass difference is generated by the two lightest neutrinos and a natural neutrino mass hierarchy can be realized if $m_1 \ll m_2$, whereas in the inverted scheme the smallest squared-mass difference is generated by the two heaviest neutrinos, which are almost degenerate for any value of the lightest neutrino mass m_3.

In the case of three-neutrino mixing there are no sterile neutrinos, in agreement with the absence of any indication in favor of active–sterile transitions in both solar and atmospheric neutrino experiments. Let us however
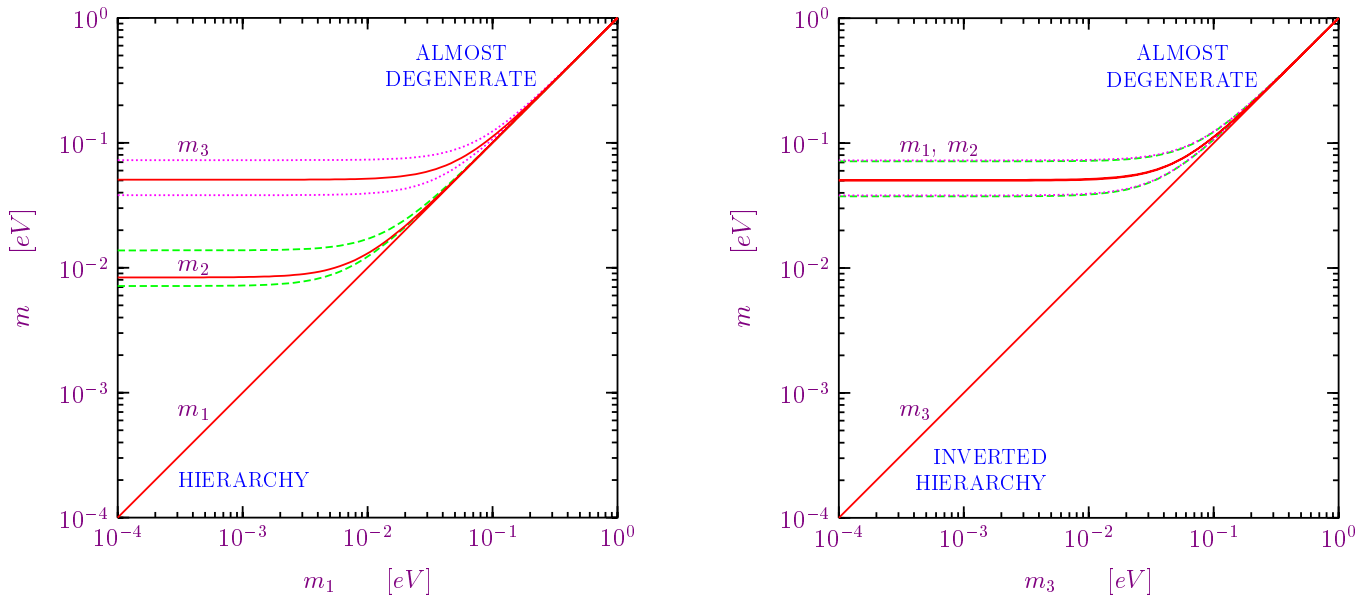
Fig. 5. Allowed ranges for the neutrino masses as functions of the lightest mass m_1 and m_3 in the normal and inverted three-neutrino scheme, respectively.

emphasize that three-neutrino mixing cannot explain the indications in favor of short-baseline $\bar{\nu}_\mu \to \bar{\nu}_e$ transitions observed in the LSND experiment [17], which are presently under investigation in the MiniBooNE experiment [18].

Let us now discuss the current information on the three-neutrino mixing matrix U. In solar neutrino experiments ν_μ and ν_τ are indistinguishable, because the energy is well below μ and τ production and ν_μ, ν_τ can be detected only through flavor-blind neutral-current interactions. Hence, solar neutrino oscillations, as well as the oscillations in the KamLAND experiment, depend only on the first row U_{e1}, U_{e2}, U_{e3} of the mixing matrix, which regulates ν_e and $\bar{\nu}_e$ disappearance. The hierarchy $\Delta m^2_{\text{SUN}} \ll \Delta m^2_{\text{ATM}}$ implies that neutrino oscillations generated by Δm^2_{ATM} in (7) depend only on the last column U_{e3}, $U_{\mu3}$, $U_{\tau3}$ of the mixing matrix, because m_1 and m_2 are indistinguishable. The only connection between solar and atmospheric oscillations is due to the element U_{e3}. The negative result of the CHOOZ long-baseline $\bar{\nu}_e$ disappearance experiment [19] implies that electron neutrinos do not oscillate at the atmospheric scale, in agreement with the above mentioned disfavoring of $\nu_\mu \to \nu_e$ transitions in atmospheric experiments. The CHOOZ bound on the effective mixing angle $\sin^2 2\vartheta_{\text{CHOOZ}} = 4|U_{e3}|^2 \left(1 - |U_{e3}|^2\right)$ implies that $|U_{e3}|$ is small: $|U_{e3}|^2 < 5 \times 10^{-2}$ (99.73% C.L.) [20]. Therefore, solar and atmospheric neutrino oscillations are practically decoupled [21] and the effective mixing angles in solar, atmospheric and CHOOZ experiments can be related to the elements of the three-neutrino mixing matrix by (see also [22])

$$\sin^2 \vartheta_{\text{SUN}} = \frac{|U_{e2}|^2}{1 - |U_{e3}|^2} \qquad \sin^2 \vartheta_{\text{ATM}} = |U_{\mu3}|^2 , \quad (8)$$

and $\sin^2 \vartheta_{\text{CHOOZ}} = |U_{e3}|^2$ Taking into account all the above experimental constraints, the best-fit value for the

mixing matrix U is

$$U_{\text{bf}} \simeq \begin{pmatrix} -0.83 & 0.56 & 0.00 \\ 0.40 & 0.59 & 0.71 \\ 0.40 & 0.59 & -0.71 \end{pmatrix} . \quad (9)$$

We have also reconstructed the allowed ranges for the elements of the mixing matrix (see [23] for a more precise reconstruction taking into account the correlations among the mixing parameters):

$$|U| \simeq \begin{pmatrix} 0.71-0.88 & 0.46-0.68 & 0.00-0.22 \\ 0.08-0.66 & 0.26-0.79 & 0.55-0.85 \\ 0.10-0.66 & 0.28-0.80 & 0.51-0.83 \end{pmatrix} . \quad (10)$$

Such mixing matrix, with all elements large except U_{e3}, is called "bilarge". It is very different from the quark mixing matrix, in which mixing is very small. Such difference is an important piece of information for our understanding of the physics beyond the Standard Model, which presumably involves some sort of quark-lepton unification.

The absolute scale of neutrino masses is not determined by the observation of neutrino oscillations, which depend only on the differences of the squares of neutrino masses. Figure 5 shows the allowed ranges (between the dashed and dotted lines) for the neutrino masses obtained from the allowed values of the oscillation parameters in (1), (2), (4), (5), as functions of the lightest mass in the normal and inverted three-neutrino schemes. The solid lines correspond to the best fit values of the oscillation parameters. One can see that at least two neutrinos have masses larger than about 7×10^{-3} eV.

The most sensitive known ways to probe the absolute values of neutrino masses are the observation of the end-point part of the electron spectrum in Tritium β-decay, the observation of large-scale structures in the early universe and the search for neutrinoless double-β decay, if neutrinos are Majorana particles (see [24]; we do not consider here the interesting possibility to determine neutrino masses through the observation of supernova neutrinos).
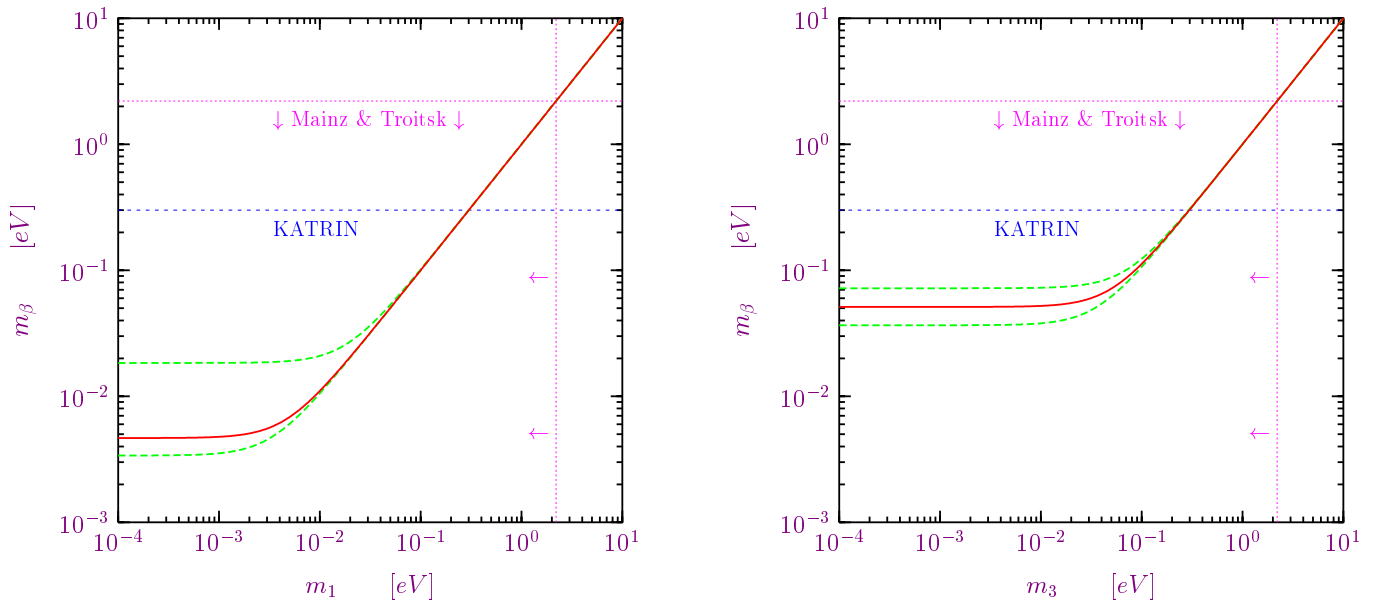
Fig. 6. Effective neutrino mass m_β in Tritium β-decay experiments as a function of the lightest mass m_1 and m_3 in the normal and inverted three-neutrino scheme, respectively.

Up to now, no indication of a neutrino mass has been found in Tritium β-decay experiments, leading to an upper limit on the effective mass

$$m_\beta = \sqrt{\sum_k |U_{ek}|^2 m_k^2} \qquad (11)$$

of $2.2\,\mathrm{eV}$ at 95% C.L. [25], obtained in the Mainz and Troitsk experiments. After 2007, the KATRIN experiment [26] will explore m_β down to about $0.2 - 0.3\,\mathrm{eV}$. Figure 6 shows the allowed range (between the dashed lines) for m_β obtained from the allowed values of the oscillation parameters in (1), (2), (4), (5), as a function of the lightest mass in the normal and inverted three-neutrino schemes. The solid line corresponds to the best fit values of the oscillation parameters. One can see that in the normal scheme with a mass hierarchy m_β has a value between about $3 \times 10^{-3}\,\mathrm{eV}$ and $2 \times 10^{-2}\,\mathrm{eV}$, whereas in the inverted scheme m_β is larger than about $3 \times 10^{-2}\,\mathrm{eV}$. Therefore, if in the future it will be possible to constraint m_β to be smaller than about $3 \times 10^{-2}\,\mathrm{eV}$, a normal hierarchy of neutrino masses will be established.

The analysis of recent data on cosmic microwave background radiation and large scale structure in the universe in the framework of the standard cosmological model has allowed to establish an upper bound of about 1 eV for the sum of neutrino masses, which implies an upper limit of about 0.3 eV for the individual masses [27,28]. This limit is already at the same level as the sensitivity of the future KATRIN experiment. Let us emphasize, however, that the KATRIN experiment is important in order to probe the neutrino masses in a model-independent way,

A very important open problem in neutrino physics is the Dirac or Majorana nature of neutrinos. From the theoretical point of view it is expected that neutrinos are

Majorana particles, with masses generated by effective Lagrangian terms in which heavy degrees of freedom have been integrated out (see [29]). In this case the smallness of neutrino masses is naturally explained by the suppression due to the ratio of the electroweak symmetry breaking scale and a high energy scale associated with the violation of the total lepton number and new physics beyond the Standard Model.

The best known way to search for Majorana neutrino masses is neutrinoless double-β decay, whose amplitude is proportional to the effective Majorana mass

$$|\langle m \rangle| = \left| \sum_k U_{ek}^2 m_k \right|. \qquad (12)$$

The present experimental upper limit on $|\langle m \rangle|$ between about 0.3 eV and 1.3 eV has been obtained in the Heidelberg-Moscow and IGEX experiments. The large uncertainty is due to the difficulty of calculating the nuclear matrix element in the decay. Figure 7 shows the allowed range for $|\langle m \rangle|$ obtained from the allowed values of the oscillation parameters in (1), (2), (4), (5), as a function of the lightest mass in the normal and inverted three-neutrino schemes (see also [30]). If CP is conserved, $|\langle m \rangle|$ is constrained to lie in the shadowed region. Finding $|\langle m \rangle|$ in an unshaded strip would signal CP violation. One can see that in the normal scheme large cancellations between the three mass contributions are possible and $|\langle m \rangle|$ can be arbitrarily small. On the other hand, the cancellations in the inverted scheme are limited, because ν_1 and ν_2, with which the electron neutrino has large mixing, are almost degenerate and much heavier than ν_3. Since the solar mixing angle is less than maximal, a complete cancellation between the contributions of ν_1 and ν_2 is excluded, leading to a lower bound of about $1 \times 10^{-3}\,\mathrm{eV}$ for $|\langle m \rangle|$ in the inverted scheme. If in the future $|\langle m \rangle|$ will be found to be
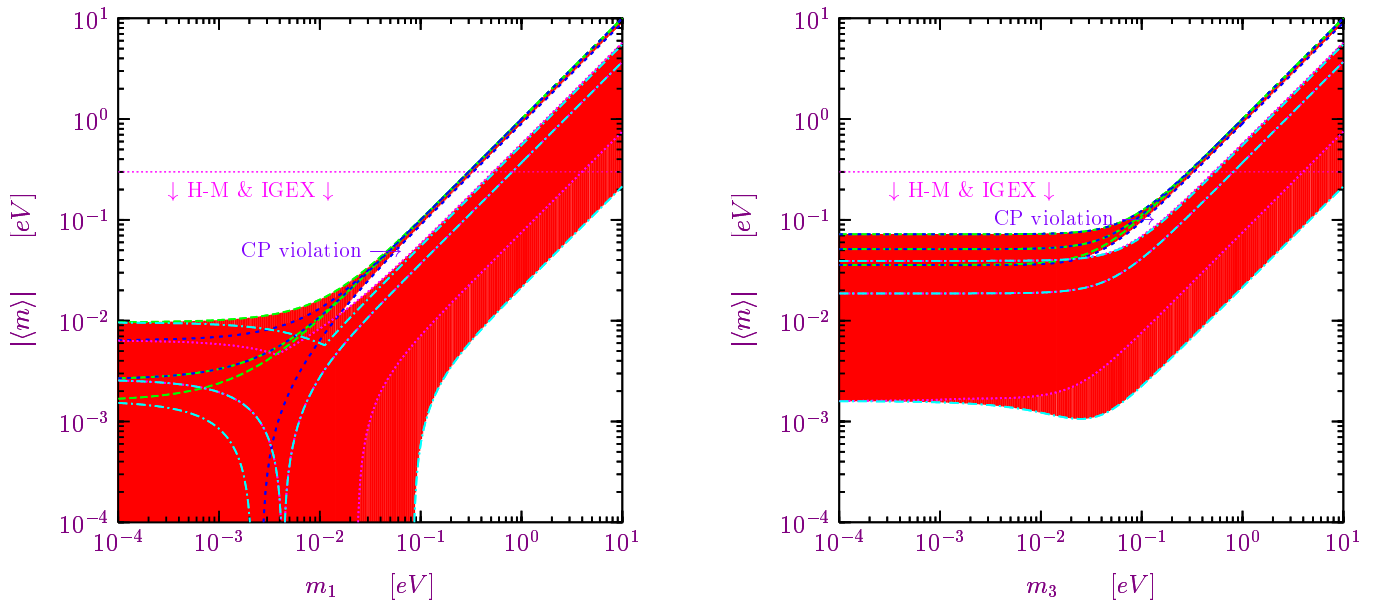
Fig. 7. Effective Majorana mass $|\langle m \rangle|$ in neutrinoless double-β decay experiments as a function of the lightest mass m_1 and m_3 in the normal and inverted three-neutrino scheme, respectively.

smaller than about 1×10^{-3} eV, it will be established that either neutrinos have a mass hierarchy or they are Dirac particles. Many neutrinoless double-β decay experiments are planned for the future, but they will unfortunately not be able to probe such small values of $|\langle m \rangle|$, extending their sensitivity at most in the 10^{-2} eV range (see [24]).

In conclusion, the recent years have been extraordinarily fruitful for neutrino physics, yielding model-independent proofs of solar and atmospheric neutrino oscillations, which have provided important information on the neutrino mixing parameters. Neglecting the controversial indications in favor of short-baseline $\bar{\nu}_\mu \to \bar{\nu}_e$ transitions observed in the LSND experiment [17], three-neutrino mixing nicely explains all data. Let us emphasize however that still several fundamental characteristics of neutrinos are unknown. Among them, the Dirac or Majorana nature of neutrinos, the absolute scale of neutrino masses, the distinction between the normal and inverted schemes, the value of $|U_{e3}|$ and the existence of CP violation in the lepton sector are very important for our understanding of the new physics beyond the Standard Model.

References

1. Q.R. Ahmad et al.: Phys. Rev. Lett. 89 (2002) 011301
2. C. Giunti and M. Laveder: hep-ph/0301276
3. K. Eguchi et al.: Phys. Rev. Lett. 90 (2003) 021802, hep-ex/0212021
4. P.C. de Holanda and A.Y. Smirnov: JCAP 0302 (2003) 001, hep-ph/0212270
5. M. Maltoni, T. Schwetz and J. Valle: Phys. Rev. D67 (2003) 093003, hep-ph/0212129
6. J.N. Bahcall, M.C. Gonzalez-Garcia and C. Pena-Garay: JHEP 0302 (2003) 009, hep-ph/0212147
7. J.N. Bahcall, M.H. Pinsonneault and S. Basu: Astrophys. J. 555 (2001) 990, astro-ph/0010346
8. K. Inoue: hep-ex/0307030
9. A. Bandyopadhyay, S. Choubey and S. Goswami: Phys. Rev. D67 (2003) 113011, hep-ph/0302243
10. J.N. Bahcall and C. Pena-Garay: hep-ph/0305159
11. S. Choubey, S. Petcov and M. Piai: hep-ph/0306017
12. G. Fogli et al.: Phys. Rev. D 67 (2003) 093006, hep-ph/0303064
13. Y. Fukuda et al.: Phys. Rev. Lett. 81 (1998) 1562, hep-ex/9807003
14. M.H. Ahn et al.: Phys. Rev. Lett. 90 (2003) 041801, hep-ex/0212007
15. T. Nakaya: hep-ex/0209036
16. S.M. Bilenky, C. Giunti and W. Grimus: Prog. Part. Nucl. Phys. 43 (1999) 1, hep-ph/9812360
17. A. Aguilar et al.: Phys. Rev. D64 (2001) 112007, hep-ex/0104049
18. A. Bazarko: hep-ex/0210020
19. M. Apollonio et al.: Eur. Phys. J. C 27 (2003) 331, hep-ex/0301017
20. G.L. Fogli et al.: Phys. Rev. D 66 (2002) 093008, hep-ph/0208026
21. S.M. Bilenky and C. Giunti: Phys. Lett. B 444 (1998) 379, hep-ph/9802201
22. W.L. Guo and Z.Z. Xing: Phys. Rev. D 67 (2003) 053002, hep-ph/0212142
23. M.C. Gonzalez-Garcia and C. Pena-Garay: hep-ph/0306001
24. S.M. Bilenky et al.: Phys. Rept. 379 (2003) 69, hep-ph/0211462
25. C. Weinheimer: hep-ex/0210050
26. A. Osipowicz et al.: hep-ex/0109033
27. D.N. Spergel et al.: astro-ph/0302209
28. S. Hannestad: astro-ph/0303076
29. G. Altarelli and F. Feruglio: hep-ph/0306265
30. S. Pascoli, S.T. Petcov and W. Rodejohann: Phys. Lett. B549 (2002) 177, hep-ph/0209059